






Evaluating the effects of azelaic acid in the metabolism of *Arabidopsis thaliana* seedlings through untargeted metabolomics and ionomics approaches

Sara Álvarez-Rodríguez^{1,2}  | Biancamaria Senizza³  | Fabrizio Araniti⁴  |
Luigi Lucini³  | Giorgio Lucchini⁴ | Adela M. Sánchez-Moreiras^{1,2} 

¹Universidade de Vigo. Departamento de Biología Vexetal e Ciencias do Solo, Facultade de Biología, Vigo, Spain

²Instituto de Agroecoloxía e Alimentación (IAA), Universidade de Vigo - Campus Auga, Ourense, Spain

³Department for Sustainable Food Process, CRAST Research Centre, Università Cattolica del Sacro Cuore, Piacenza, Italy

⁴Dipartimento di Scienze Agrarie e Ambientali - Produzione, Territorio, Agroenergia, Università Statale di Milano, Milano, Italy

Correspondence

Corresponding authors,
Adela M. Sánchez-Moreiras,
Email: adela@uvigo.gal

Funding information

Xunta de Galicia, Grant/Award Number: ED481A-2021/328; MCIN/AEI/10.13039/501100011033, Grant/Award Number: RT12018-094716-B-100; HORIZON EUROPE Framework Programme, Grant/Award Number: 101084084

Edited by S. Martens

Abstract

The present study demonstrates that low concentrations of azelaic acid (AZA) significantly impact the metabolism of *Arabidopsis thaliana* seedlings, leading to imbalances in numerous minerals and metabolites due to AZA-induced stress. Untargeted metabolomic analyses were conducted on untreated and AZA-treated seedlings at two time points: 7 and 14 days after treatment initiation. The results revealed a general accumulation of sugars (e.g., glucose, mannose, xylose), amino acids (e.g., lysine, GABA, threonine, glutamine), and organic acids (e.g., glutaric acid, shikimic acid, succinic acid) in AZA treated-seedlings, suggesting that AZA triggers stress responses in *Arabidopsis*. Ionomics analysis revealed that AZA induces phosphorus deficiency, which plants compensate by increasing malate content in the roots. Additionally, AZA treatment induced putrescine accumulation within the root, a metabolic biomarker of potassium deficiency and plant stress. The metabolomic profile showed elevated levels of different specialized metabolites, such as nitrogen- and sulphur-containing compounds, and altered levels of various phytohormones, including jasmonates and brassinosteroids, implicated in plant protection under biotic and/or abiotic stresses. These findings support the hypothesis that AZA's mode of action is associated with an auxin imbalance, suggesting its function as an auxinic herbicide. The observed increases in starch and jasmonates, coupled with the disruptions in potassium homeostasis, are linked to the previously reported alterations in the auxin transport, root architecture and gravitropic root response. Statistical analyses were applied, including Kruskal-Wallis tests for ionomics data, as well as multifactor analysis, Principal Component Analysis, Orthogonal Partial Least Squares-Discriminant Analysis, and enrichment pathway analysis for metabolomic data, ensuring the robustness and validity of these findings.

This is an open access article under the terms of the [Creative Commons Attribution-NonCommercial-NoDerivs](https://creativecommons.org/licenses/by-nc-nd/4.0/) License, which permits use and distribution in any medium, provided the original work is properly cited, the use is non-commercial and no modifications or adaptations are made.

© 2024 The Author(s). *Physiologia Plantarum* published by John Wiley & Sons Ltd on behalf of Scandinavian Plant Physiology Society.

1 | INTRODUCTION

The number of herbicide-resistant weed species has increased by around 500% in the last 30 years, whereas no herbicides with innovative sites of action have been commercialized (Dayan & Duke, 2020). Identifying new molecules from diverse sources, including plant extracts, microorganisms, or synthesized compounds, has gained interest among researchers, as they can be considered environmentally friendly alternatives to traditional chemical herbicides (Qu et al., 2021). Discovering insights about changes occurring in plant metabolism can help in elucidating new modes of action, since plant metabolism is implicated in biochemical processes within the plant, including plant growth, development, or responses to environmental stimuli.

Dicarboxylic acids are promising compounds among a plethora of plant specialized metabolites with potential applications in sustainable weed management. Researchers have already studied the phytotoxic potential of the exogenous application of several dicarboxylic acids, including oxalic, adipic, succinic, and malonic acids. For instance, Hirabayashi et al., (2001) reported that succinic and adipic acid exhibited phytotoxicity against tobacco plants, impacting growth and leaf development. Wu et al., (2011) also demonstrated that high concentrations of succinic acid inhibited the growth and conidia germination of *Fusarium oxysporum* f. sp. *niveum*. These findings underscore the potential of dicarboxylic acids as natural herbicidal agents. However, with the escalating issue of herbicide-resistant weeds, the demand for innovative and effective herbicidal solutions has never been more urgent. In this context, azelaic acid (AZA) emerges as a particularly interesting candidate for further investigations.

Azelaic acid (AZA) is a saturated dicarboxylic acid that can be naturally found in certain grains such as rye, barley, or wheat, and it is also produced by organisms such as the fungus *Malassezia furfur*. Although AZA's biocide potential is well-known for its efficacy in the treatment of rosacea, hyperpigmentation disorders, or acne vulgaris due to its antibacterial and anti-inflammatory activities (Spaggiari et al., 2023), little information is available regarding the possible phytotoxic potential of this compound. For example, Ma et al., (2011) demonstrated that extracts of leaves and roots of *Jatropha curcas*, mainly composed of azelaic acid, inhibited germination, shoot, and root growth of *Zea mays* L., suggesting a competitive defense strategy of *J. curcas* against neighboring crops. Dong et al., (2019) also revealed that azelaic acid was one of the active allelopathic substances from *C. demersum* extracts, favoring the growth of the alga *C. vulgaris*. A recent study revealed that AZA has strong phytotoxic activity against *Arabidopsis thaliana* seedlings (Álvarez-Rodríguez et al., 2024). An initial investigation into the mode of action of this molecule in plant metabolism was conducted in that study, providing insights into the alterations induced by AZA on root growth, morphology, and anatomy, auxin transport, and potential target proteins affected by this molecule.

Due to its proven phytotoxic effects, this specialized metabolite shows potential as a promising candidate for further research into its use as a bioherbicide in weed control. Enhancing our comprehension

of the mechanisms through which natural compounds exert phytotoxic effects within plants is paramount for acquiring comprehensive insights into their specific target sites of action (Araniti et al., 2020; López-González et al., 2023; Misra et al., 2020). Conducting innovative metabolomic approaches can be an effective tool for acquiring extensive information about metabolites and understanding the metabolic pathways influenced by these phytotoxic natural compounds.

Metabolomics is considered as a novel technique that provides valuable information about the metabolic pathways within the plant. Metabolic pathways refer to the interconnected reactions that regulate the flow of metabolites within a cell. Therefore, conducting accurate metabolome analyses can reveal insights into the diverse defense mechanisms employed by plants to survive under different stress situations (Salam et al., 2023). Osmoprotectants, a subset of metabolites, play a crucial role in helping plants to face different stress situations, particularly in those responses related to abiotic stress conditions such as drought, high temperatures, or salinity. Under severe conditions, changes in the concentration of these compounds at the cellular level depend on diverse factors, including the stress intensity and duration, the plant species, or the growth conditions (Zulfiqar et al., 2020). Their accumulation usually facilitates multiple functions, including osmotic adjustment through regulating cell turgor pressure, replacing inorganic ions, protecting biological membranes, or detoxifying ROS, among others. Examples of osmoprotectants include compound groups such as amino acids e.g., proline, alanine, GABA, organic acids e.g., malic acid, fumaric acid, sugars e.g., trehalose, sucrose, mannose, or sugar alcohols e.g., inositol, mannitol (Slama et al., 2015).

In addition, ionomics is considered the study of the elemental composition of different organisms, determining how the environment influences the mineral composition of target tissues, cells, or individuals (Pita-Barbosa et al., 2019). In the case of plants, the combination of metabolomics and ionic techniques can complement each other and provide insights into the plants' ability to respond to various environmental stress situations (Kumari et al., 2015). For this reason, in this study, we performed an untargeted metabolomic analysis and an ionic analysis at different times, revealing important information about the alterations occurring within the plant metabolism in *A. thaliana* seedlings after azelaic acid treatment.

2 | MATERIALS AND METHODS

2.1 | Plant material and growth conditions

Seeds of *Arabidopsis thaliana* (L.) Heynh. ecotype Columbia (Col-0) were sterilized according to the following steps: 3 min in 50% ethanol, 3 min in 0.5% NaOCl (supplemented with 0.01% Triton x100), three washes in sterile water, and finally 48 h in 0.1% sterile agar at 4°C. Afterwards, the seeds were sown in square Petri dishes containing 0.8% plant agar, 0.44% Murashige-Skoog

nutrients (Sigma-Aldrich) and 1% sucrose. Then, plates were placed vertically in a growth chamber with the following conditions: 16 hours light / 8 hours darkness, $22 \pm 2^\circ\text{C}$ constant temperature, and 55% relative humidity. Azelaic acid was dissolved in ethanol (0.01%), and the corresponding amount was added to the plant agar solution to reach the desired concentration (44 μM), based on previous phytotoxic studies with this molecule on *A. thaliana* seedlings (Álvarez-Rodríguez et al., 2024). Control samples were prepared using the same concentration of ethanol (0.01%) without azelaic acid, to account for any potential effects of the solvent itself. Depending on the experiment, plant material was collected after 7 and/or 14 days of growth.

2.2 | Mineral composition by ICP-MS ionic analysis

For ionic analysis, the mineral content of untreated and IC₅₀ (44 μM) AZA-treated plants was compared after 14 days of growth. A pool of plant material was collected and dried at 70°C for 72 h. After this time, four replications of 100 mg were selected per treatment, and the procedure was done according to Álvarez-Rodríguez et al., (2023b). The concentration of magnesium (Mg^{2+}), potassium (K^+), sodium (Na^+), cobalt (Co^{2+}), copper (Cu^{2+}), iron ($\text{Fe}^{2+} + 3+$), calcium (Ca^{2+}), manganese ($\text{Mn}^{2+} + 3+$), selenium (Se^{2-}), phosphorus (P^{3-}), arsenic (As^{3-}) and zinc (Zn^{2+}) was measured.

2.3 | Metabolite extraction and analytical profiling

2.3.1 | GC-MS-driven untargeted metabolomics

For GC-MS-driven metabolomic analysis, sample extractions and derivatizations were carried out following the protocol proposed by Lisec et al., (2006) and modified by Álvarez-Rodríguez et al., (2023a). Ribitol was used as internal standard (0.2 mg ml⁻¹), and samples were injected into an Agilent gas chromatograph apparatus (GC 7890A) equipped with a single quadrupole mass spectrometer (MS 5975C INERT XL MSD) and a CTC ANALYTICS PAL autosampler. The column MEGA-5MS (30 m \times 0.25 mm \times 0.25 μm + 10 m pre-column; MEGA s.r.l.) was employed, and 1 μL of each sample was injected with a helium flow of 1 mL min⁻¹. At specified intervals, qualitative controls (QCs), *n*-alkane standards (C8-C40 all even) and blank samples (pyridine, methoxyamine hydrochloride, and MSTFA) were injected to assess instrumental performance, make provisional identifications, and monitor changes in retention indices (RI). The temperature ramp to achieve metabolite separation and the successive sample alignment, deconvolution, and peak annotation were performed according to Álvarez-Rodríguez et al., (2023a). For metabolite annotation and EI-MS spectra assignment, we followed the MSI guideline, according to Sansone et al., (2007). The Level 2 of identification was based on matching the mass spectrum to a spectral database with a high degree of similarity (match factor > 80%).

2.3.2 | UHPLC-ESI/QTOF profiling

For the metabolic profile, 100 mg per replicate were collected, and samples were extracted in an aqueous solution consisting of 80% (v/v) methanol acidified with 0.1% (v/v) formic acid through an Ultraturrax (IkaT10). Then, the tubes were centrifuged at 7 745 g (Eppendorf Centrifuge 5430, Thermo Fisher Scientific), and the supernatants were filtered through 0.22 μm regenerated cellulose (RC) filters into vials for UHPLC-ESI/QTOF analysis.

The 1290 UHPLC chromatograph was equipped with a binary pump and a Dual Electrospray JetStream ionization source, coupled to a hybrid QTOF mass analyser (G6550 mass spectrometer, Agilent Technologies). The chromatographic separation was achieved under a water-acetonitrile (both LC-MS grade) gradient elution (6–94% acetonitrile in 32 min), flow rate of 0.2 mL min⁻¹, and injection volume of 6 μL , on an Agilent Zorbax Eclipse plus C18 analytical column (50 \times 2.1 mm, 1.8 μm). The QTOF mass analyzer operated in positive mode (ESI+), full scan mode was performed within a range of the *m/z* 100–1200 (1 spectra/s). The processing of the chromatograms was carried out using the MassHunter Qualitative Analysis software (version B.06.00, Agilent Technologies). The raw mass features processing was achieved using the software Profinder B.07 (Agilent Technologies), based on “find-by-formula” algorithm. In this regard, compound annotation was recursively achieved, following mass and retention time alignment, using the Plantcyc database. The annotation was based on the isotopic profile of each molecular feature detected, consisting of a monoisotopic mass, isotope spacing, and ratio combination, with a mass accuracy of 5 ppm. The identification of putatively annotated compounds was conducted following the Confidence Level 2 of the Metabolomics Standards Initiative (MSI), in accordance with COSMOS standards in metabolomics (Salek et al., 2013).

2.4 | Statistical analysis

Metabolomic analyses were conducted with five replications per treatment, while the ionic analysis was performed with four replications. Data from the ionic analysis were analyzed through a Kruskal-Wallis' test ($p \leq 0.05$). For the GC/MS metabolomic analysis, the raw data were normalized on MS-DIAL software using the Internal Standard Ribitol. Statistical analysis was performed in Metaboanalyst 6.0, applying ‘Log₁₀ transformation’ and ‘Pareto scaling’ to the data. A multifactor analysis was first conducted to evaluate the data. The interactive unsupervised Principal Component Analysis (PCA 3D) was carried out to discriminate and classify the data. Subsequently, a two-way analysis of variance (ANOVA) and a Pattern Hunter correlation analysis were employed to evaluate the trends and interactions between the two variables (Treatment and Days of Treatment).

In the second step, the data were separately analyzed (dividing 7 from 14 days of treatment) to further evaluate the effects of the treatment individually. The Orthogonal Partial Least Squares-Discriminant Analysis (OPLS-DA) was performed to visualize the sample group differentiation, and the VIP analysis (variable importance in

projection) was used to identify the metabolites contributing to sample group separation. The accuracy of the model was confirmed through a validation process ($p \leq 0.05$; Figure S1). The data were analyzed through a univariate t -test ($p \leq 0.05$) and represented through violin plots. Finally, an enrichment pathway analysis was conducted to identify the alterations within the networks. A False Discovery Rate (FDR) was applied to the nominal p -values. All raw data is available in Supplementary Table S1.

For the metabolic UHPLC-ESI/QTOF profiling, Mass Profiler Professional 15.1 software (Agilent Technologies) was employed for data filtration (area threshold $>10,000$ counts), Log_2 -transformation, and normalization at the 75th percentile. Detected features were baselined to their median in the dataset. Unsupervised hierarchical cluster analysis (HCA) was conducted and normalized data were Pareto-scaled for multivariate data analysis by SIMCA[®] version 17 software (Sartorius). Supervised Orthogonal Partial Least Squares-Discriminant Analysis (OPLS-DA) was conducted. The goodness-of-fit (R2Y) and the goodness-of-prediction (Q2Y) parameters were calculated to evaluate the quality of the models. The differential metabolites were identified by combining ANOVA (P -value <0.05 , Bonferroni multiple testing correction) and fold-change (\log Fold Change ≥ 1.2) through the Volcano Plot analysis. The significant compounds were then considered for the pathway analysis using the Omic Viewer Pathway Tool of PlantCyc (Stanford) for biochemical interpretations. All raw data are available in Supplementary Table S2.

3 | RESULTS

3.1 | Impact of azelaic acid treatment on the ionic profile of *A. thaliana* seedlings

After 14 days of treatment, AZA negatively altered the ionic profile of *A. thaliana* seedlings. Results revealed that AZA strongly reduced the concentrations of Co^{2+} (90% lower), $\text{Fe}^{2+} + ^{3+}$ (70% lower), P^{3-} (62% lower), and Zn^{2+} (60% lower) when compared to control values, while K^+ (26% lower), Mg^{2+} (16% lower), Na^+ (15% lower), and Ca^{2+} (11% lower) were less but also significantly reduced when compared to untreated seedlings. On the contrary, ions such as Cu^{2+} , $\text{Mn}^{2+} + ^{3+}$, As^{3-} and Se^{2-} were not significantly affected by AZA treatment (Table 1).

3.2 | Effects of azelaic acid treatment in the *A. thaliana* metabolome

The GC/MS-driven untargeted metabolomic analysis carried out in MSDIAL, identified a total of 310 compounds, of which 153 were considered unknown and 157 were putatively annotated. After discarding false annotated metabolites, a total of 86 metabolites were finally annotated. Then, the data were normalized using the Internal Standard, and a statistical analysis was performed using Metaboanalyst 6.0.

TABLE 1 Mineral contents of *A. thaliana* seedlings untreated or treated with the IC_{50} AZA (44 μM) after 14 days of treatment. Data are expressed in μg element per g of dry weight of each sample (parts per million). Asterisks indicate significant differences between control and AZA-treated seedlings after a Kruskal-Wallis' test.

* $p \leq 0.05$. $n = 4$.

Element ($\mu\text{g g}^{-1}$ DW)	Control	IC_{50} AZA
Na^+	1262.41 \pm 69.03	1076.87 \pm 27.09 *
Mg^{2+}	2438.29 \pm 90.48	2034.78 \pm 38.36 *
K^+	66322.86 \pm 3571.83	49093.37 \pm 505.49 *
Ca^{2+}	5751.87 \pm 324.60	5123.05 \pm 88.39 *
$\text{Fe}^{2+} + ^{3+}$	1031.12 \pm 113.80	317.38 \pm 20.32 *
Co^{2+}	0.31 \pm 0.16	0.06 \pm 0.07 *
Zn^{2+}	283.16 \pm 19.79	119.91 \pm 4.04 *
P^{3-}	12487.02 \pm 483.69	4766.53 \pm 71.72 *
As^{3-}	0.26 \pm 0.38	0.02 \pm 0.06
Se^{2-}	2.51 \pm 0.96	3.77 \pm 0.47
Cu^{2+}	5.31 \pm 2.21	3.05 \pm 0.78
$\text{Mn}^{2+} + ^{3+}$	253.28 \pm 18.43	233.96 \pm 5.28

3.2.1 | Global comparative metabolomics analysis

Firstly, the data were collectively analyzed, considering the two evaluated variables: Treatment (control or AZA-treated seedlings) and Days of Treatment (7 or 14 days). The Unsupervised Principal Component Analysis (PCA) demonstrated a perfect separation between sample groups for both, treatment and time (Figure 1 A, B). In this context, due to the multivariate analysis, the 3D PCA Score plots are useful for visualizing the distribution of variance across three dimensions, allowing for a more detailed understanding of the data structure. The PCA 3D Score plots, built on the first (PC1), second (PC2) and third (PC3) component, got to explain an 85.6% of the total variance (Figure 1A-B). The PC1 explained a 47.2%, the PC2 explained a 9.3% and the PC3 explained a 9.1% (Figure 1). The loading plots pointed that PC1 was mainly influenced by galactinol, L-proline, inositol, aconitic acid, L-iditol and phosphoric acid, among others. In contrast, the PC2 was characterized by glutaric acid, oleic acid, glutamine, ascorbic acid, phosphoric acid, and glycerol (Supplementary Table S1).

Successively, a two-way ANOVA was conducted considering treatment (control and AZA) and days of treatment (7 and 14). The analysis revealed that both factors influenced the metabolome since 74 metabolites were significantly altered (Figure 2; the complete list is available in Supplementary Table S1). The Venn diagram revealed that 1,4 benzene dicarboxylic acid, pyrrole-2-carboxylic acid, 3-aminoisobutyric acid, 1,6 anhydro- β -D-Glucose, lauric acid, 5,6-dihydrouracil and glutaric acid were the metabolites affected only by the variable 'treatment' (Figure 2A). However, the metabolites tyrosine, methanol phosphate, melibiose, 1-docosanol, 3-amino-2-piperidone, and xylonic acid were only affected by the factor 'Days of Treatment'. Icosanoic acid was the only metabolite whose

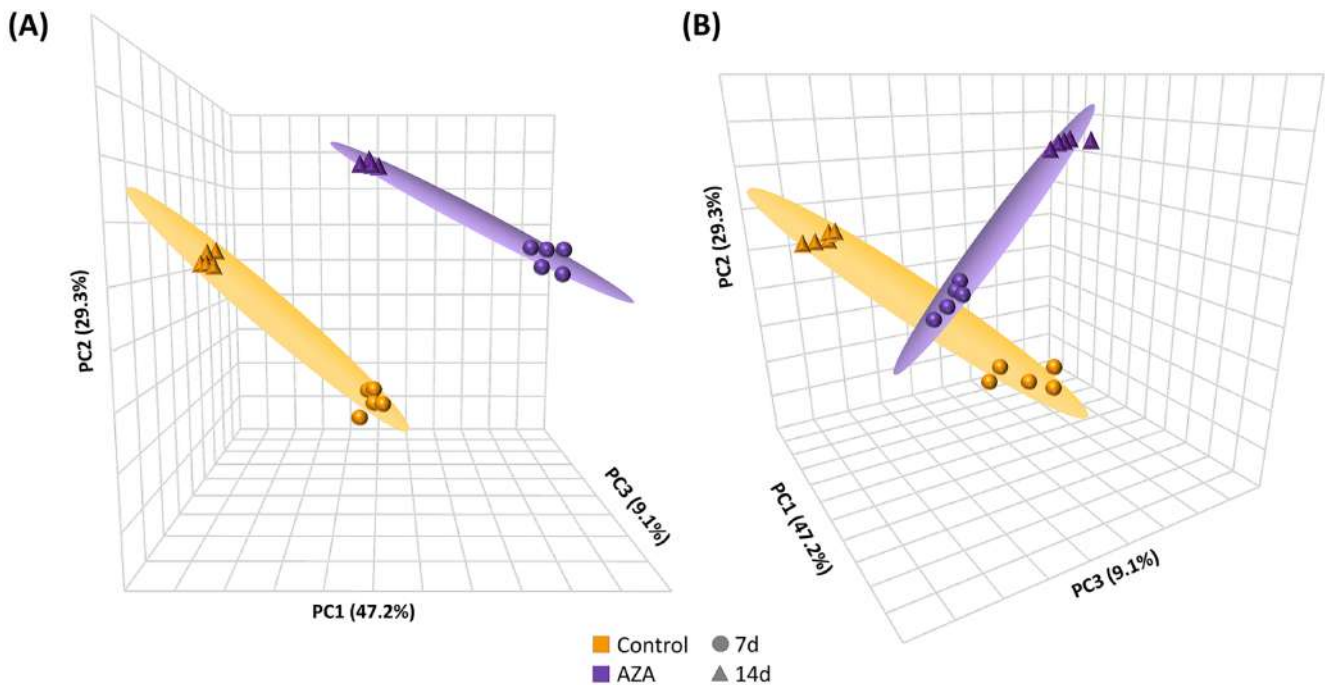


FIGURE 1 Graphical representation of Synchronized 3D Score Plots of Interactive Principal Component Analysis (PCA). (A) and (B) Separation between sample groups from different perspectives. Control group samples are represented in orange, and azelaic acid (AZA) group samples are represented in purple. Circles indicate seven days of treatment (7 d), and triangles indicate 14 days of treatment (14 d). The PCA explains 85.6% of the total variance, with 47.2% for PC1, 29.3% for PC2 and 9.1% for PC3. $n = 5$.

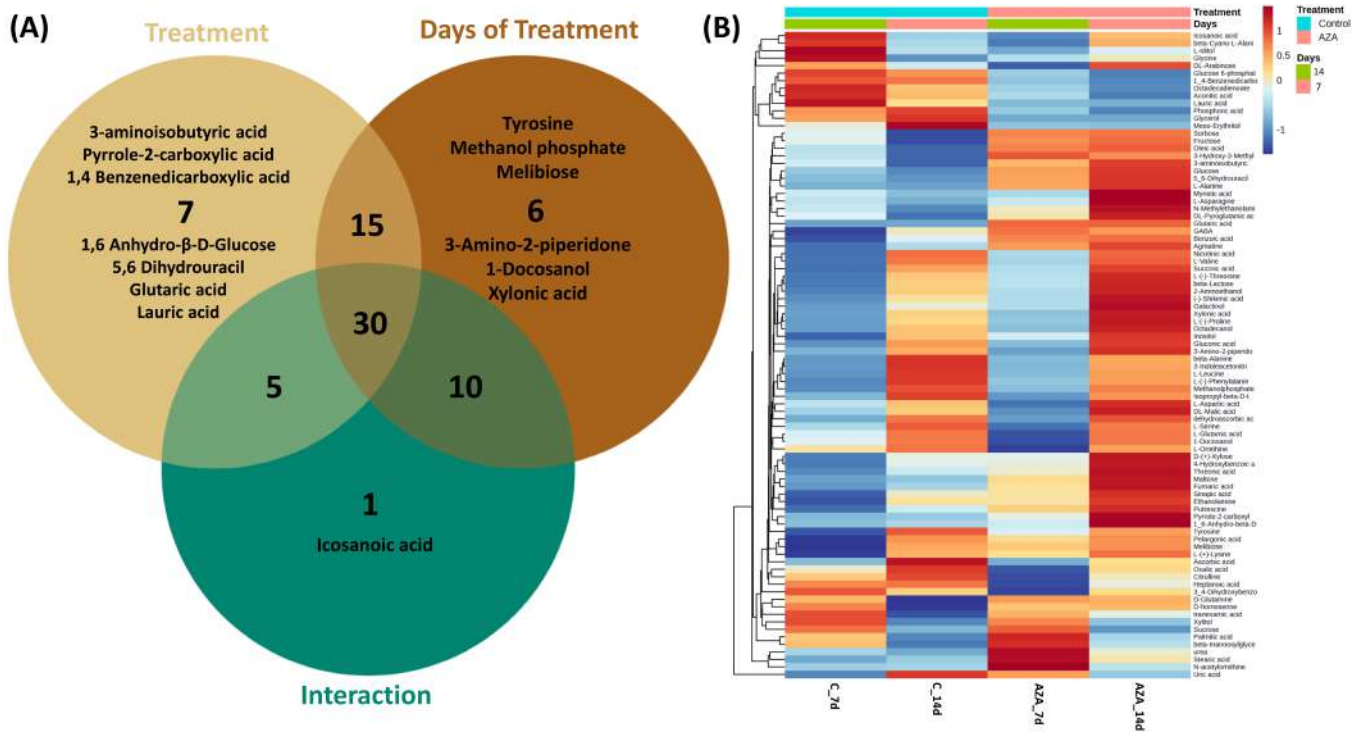


FIGURE 2 Graphical representation of (A) Venn diagram illustrating only the significantly altered metabolites after two-way ANOVA ($p < 0.05$), and (B) Heatmap showing all the identified metabolites across treatments following the metabolomic analysis. The comparison involves two variables: Treatment (control and azelaic acid-AZA) and Days of Treatment (7 and 14). $n = 5$.

alteration depended on the interaction between both factors (treatment and days of treatment). Generally, there was a good separation between sample groups, as evidenced in the heatmap (Figure 2B).

In addition, Pattern Hunter correlation analyses were performed to evaluate the relationships between the pair of variables (Treatment and Days of Treatment; Figure 3). The correlation matrices show the

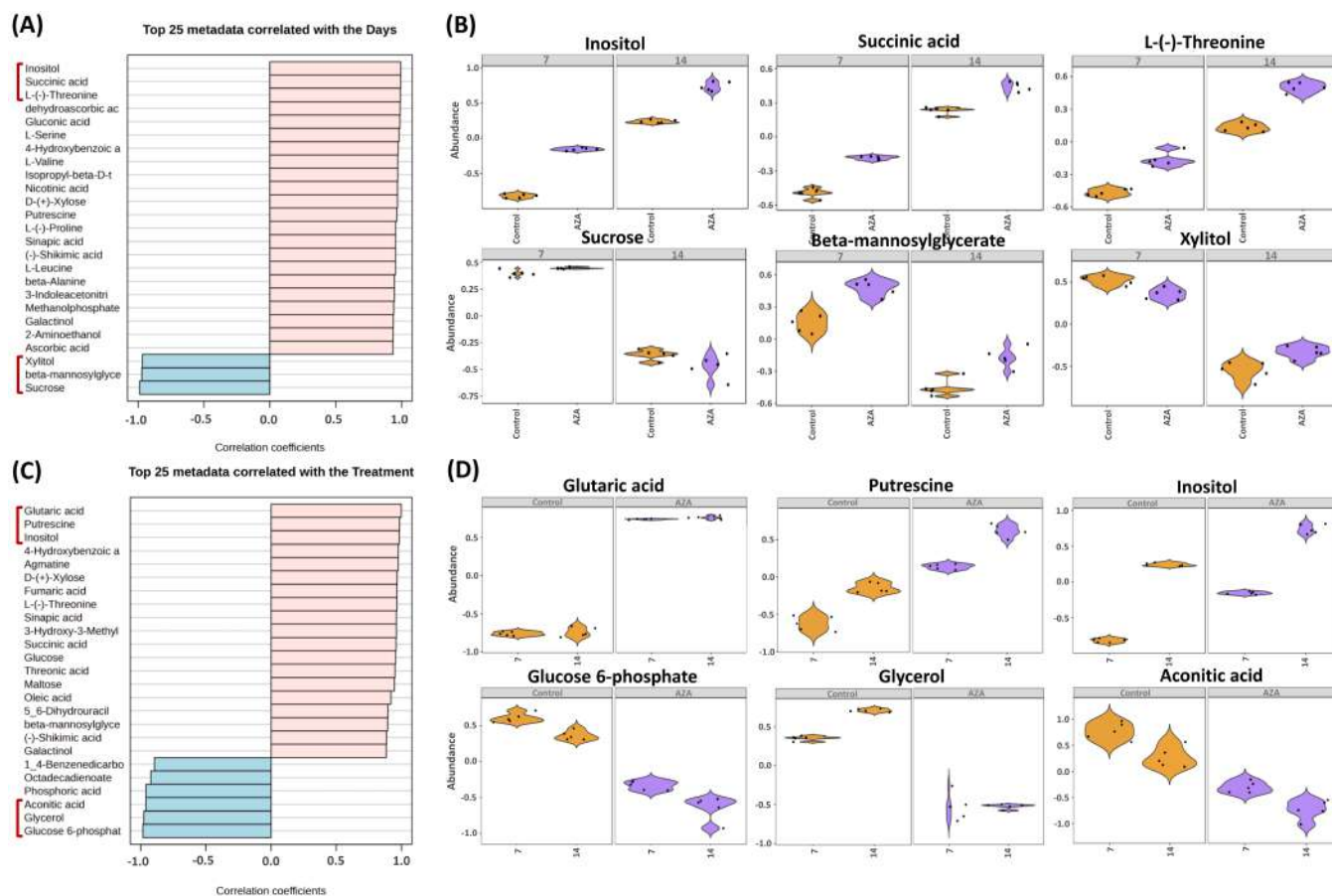


FIGURE 3 Pattern Hunter analysis between the two variables of interest: Days of Treatment (7 and 14) and Treatment (control and azelaic acid-treated seedlings). (A) Pattern hunter profile presenting the top 25 metabolites correlated with the variable ‘Days of Treatment’. (B) Graphical representation of the top three metabolites with the highest positive and negative correlation coefficients regarding the variable ‘Days of Treatment’. (C) Pattern hunter profile presenting the top 25 metabolites correlated with the variable ‘Treatment’. (D) Graphical representation of the top three metabolites with the highest positive and negative correlation coefficients regarding the variable ‘Treatment’. In the correlation graphics (A) and (C), metabolites with correlation coefficients ranging from 0 to 1 are represented in pink, indicating a positive relationship between variables, whereas correlation coefficients ranging from -1 to 0 are represented in blue, indicating a negative relationship. Violin plots depict the control group in orange and the azelaic acid (AZA) group in purple. $n = 5$.

top 25 metabolites with stronger correlation coefficients (Figure 3A, C). If the correlation coefficients of the metabolites range from 0 to 1, it indicates a positive relationship between variables, whereas correlation coefficients ranging from -1 to 0 indicate negative relationships between the two variables. The closer the correlation coefficient value is to 1, the stronger the linear relationship.

In the case of the top metabolites correlated with the variable ‘Days of Treatment’, inositol, succinic acid, and L-threonine exhibited the highest positive correlation. This suggests that as treatment time increased, these metabolites also increased for each treatment. Conversely, sucrose, β -mannosylglycerate, and xylitol showed the strongest negative correlation among variables. This indicates that as treatment time increased, the levels of these metabolites decreased for each treatment (Figure 3B). On the contrary, concerning the top metabolites correlated with the variable ‘Treatment’, glutaric acid, putrescine, and inositol showed the highest positive correlation. This implies that when plants were treated with AZA, the levels of these

metabolites increased at both 7 and 14 days. In contrast, glucose 6-phosphate, glycerol, and aconitic acid showed the strongest negative linear correlation since their coefficient values were close to -1 , which means that AZA treatment induced a reduction of these metabolites at both 7 and 14 days (Figure 3D).

3.2.2 | Specific comparative metabolomic analysis

Data from different timing points were analyzed separately to examine further alterations in the plant metabolome of AZA-treated *A. thaliana* seedlings individually. The two different treatments, control and AZA-treated seedlings, were firstly compared at 7 and then at 14 days of growth. The Orthogonal Partial Least Square Discriminant Analysis (OPLS-DA) confirmed the complete separation between sample groups (control and AZA-treated seedlings) at both, 7 and 14 days of treatment (Figure 4A, B). After 7 days, the OPLS-DA, constructed with the first two components, explained 69.7% of the total

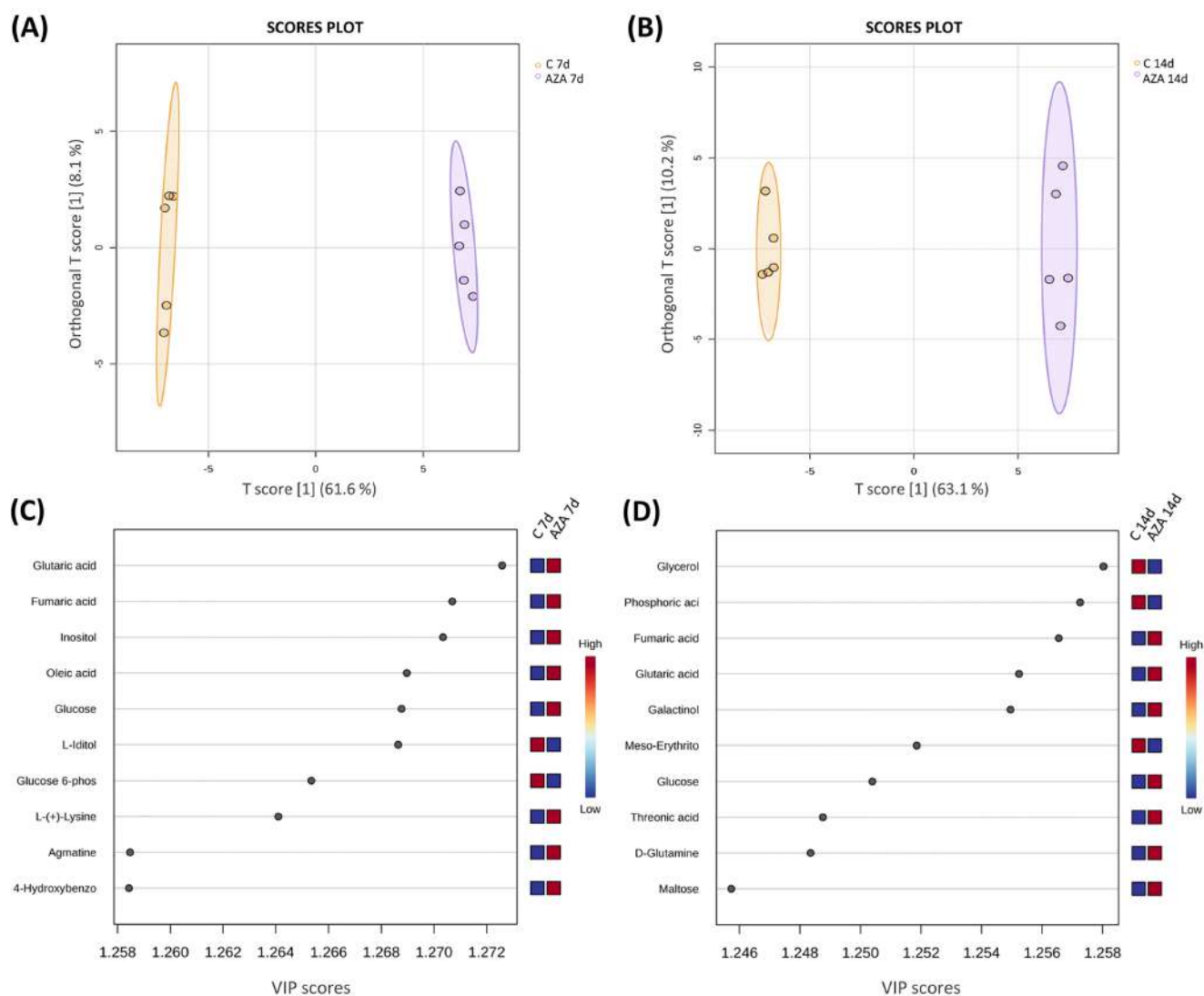


FIGURE 4 Orthogonal Partial Least Squares-Discriminant Analysis (OPLS-DA). (A) Graphical representation of untreated and AZA-treated seedlings after 7 days of growth. (B) Graphical representation of untreated and AZA-treated seedlings after 14 days of growth. (C) Variable importance of projection (VIP) features for untreated and AZA-treated seedlings after 7 days of growth. (D) Variable importance of projection (VIP) features for untreated and AZA-treated seedlings after 14 days of growth. In the OPLS-DA, the control group is represented in orange, and the azelaic acid (AZA) group is represented in purple. The accuracy of the model was confirmed through a validation process ($p \leq 0.05$). $n = 5$.

variance (PC1–61.6% and PC2–8.1%; Figure 4A). The OPLS-DA derived VIP scores based on the top 10 metabolites with highest VIP score, pointed that glutaric acid, fumaric acid, inositol, and oleic acid, among others, had the highest VIP scores (Figure 4C). In contrast, after 14 days of treatment, the OPLS-DA explained 73.2% of the total variance (PC1–63.1% and PC2–10.2%; Figure 4B). Glycerol, phosphoric acid, fumaric acid, glutaric acid, and galactinol, among others, were the metabolites with the highest VIP scores after 14 days of treatment (Figure 4D).

A *t*-test analysis revealed that 58 metabolites were significantly altered between control and AZA-treated seedlings after 7 days of growth. Meanwhile, 61 metabolites showed significant alterations after 14 days (Supplementary Table S1). The metabolites affected by AZA treatment mainly belong to sugars, amino acids, organic acids,

sugar acids and sugar alcohols, among others (Table 2). Specifically, AZA induced a significant accumulation of sugars such as glucose, xylose, maltose, sorbose and fructose after 7 and 14 days of treatment. Regarding amino acids, AZA increased lysine, GABA, threonine, L-proline and L-glutamine levels at both 7 and 14 days, whereas ornithine, glycine and L-serine levels significantly decreased. AZA increased the levels of L-valine and L-alanine in just 7 days of treatment. Aspartic acid and β -cyanoalanine were accumulated after 7 days but reduced after 14 days of AZA treatment, and glutamic acid was only significantly reduced after 7 days (Table 2). Regarding organic acids, AZA induced a stable and significant accumulation of glutaric, fumaric, shikimic, succinic and gluconic acids over time, while aconitic acid significantly decreased after AZA treatment. The behavior of malic acid changed over time, as its level decreased after

TABLE 2 List of metabolites significantly affected by azelaic acid (AZA) treatment after 7 and 14 days of growth with this natural compound. Data were analysed through t-test (p -value ≤ 0.05). A negative value of the t -stat indicates a significant increase in that specific metabolite, whereas a positive value of the t -stat indicates a significant decrease in that specific metabolite. A False Discovery Rate (FDR) was applied to the nominal p -values. AZA-7d: plants treated with AZA for 7 days; AZA-14d: plants treated with AZA for 14 days. $n = 5$.

Class	Metabolites	AZA-7d		AZA-14d	
		t-stat	p-value	t-stat	p-value
Sugars	Fructose	-5.5923	0.00051485	-9.2346	1.53E-05
	Glucose	-32.454	8.86E-10	-24.121	9.30E-09
	Glucose 6-phosphate	23.994	9.70E-09	12.649	1.43E-06
	Maltose	-10.604	5.47E-06	-21.597	2.23E-08
	Sorbose	-6.1945	0.00026099	-7.9195	4.70E-05
	Sucrose	-3.5058	0.0080108	//	//
	Xylose	-12.976	1.18E-06	-17.15	1.36E-07
Sugar acids	Threonic acid	-8.8555	2.09E-05	-20.688	3.12E-08
Sugar alcohols	Iditol	35.977	3.90E-10	//	//
	Inositol	-42.95	9.52E-11	-16.338	1.98E-07
	Galactinol	//	//	-42.857	9.69E-11
	Meso-Erythritol	//	//	29.211	2.04E-09
	Xylitol	4.328	0.0025188	-3.866	0.0047681
Amino acids	Lysine	-23.498	1.14E-08	-3.994	0.0039829
	GABA	-14.411	5.25E-07	-2.8654	0.020978
	Glycine	18.609	7.17E-08	-5.8798	0.0003701
	Threonine	-9.3965	1.35E-05	-13.865	7.08E-07
	β -Cyanoalanine	9.1131	1.69E-05	-5.1865	0.00083604
	L-Serine	6.4768	0.00019276	4.664	0.001615
	L-Valine	-4.0149	0.0038687	//	//
	L-Proline	-3.2096	0.012431	-11.867	2.33E-06
	L-Alanine	-2.8689	0.020865	//	//
	β -Alanine	//	//	5.1088	0.00091982
	L-Glutamine	-3.017	0.016636	-24.941	7.14E-09
	L-Asparagine	//	//	-17.666	1.08E-07
	Tyrosine	//	//	2.747	0.025175
	Aspartic acid	15.168	3.53E-07	-10.14	7.65E-06
	Glutamic acid	12.038	2.09E-06	//	//
L-Leucine	//	//	12.349	1.72E-06	
Poliamines	Ornithine	19.206	5.60E-08	4.0674	0.0035963
	Putrescine	-16.566	1.78E-07	-16.093	2.23E-07
Organic acids	Glutaric acid	-128.26	1.53E-14	-52.213	2.01E-11
	Fumaric acid	-51.062	2.40E-11	-50.617	2.57E-11
	Aconitic acid	12.289	1.79E-06	8.3793	3.12E-05
	Shikimic acid	-7.5679	6.50E-05	-8.7409	2.30E-05
	Malic acid	5.7828	0.00041319	-20.165	3.82E-08
	Succinic acid	-15.53	2.94E-07	-9.3787	1.37E-05
	Gluconic acid	-4.2152	0.0029351	-4.728	0.0014867
Carboxylic acid	1,4-Benzenedicarboxylic acid	11.686	2.62E-06	4.5587	0.001853
Phenolic acid	4-Hydroxybenzoic acid	-16.689	1.68E-07	-19.842	4.34E-08
Fatty acid	Oleic acid	-37.09	3.06E-10	-8.4106	3.04E-05
Phenylpropanoid	Sinapic acid	-14.509	4.99E-07	-7.9795	4.45E-05
Inorganic acid	Phosphoric acid	11.342	3.29E-06	63.086	4.43E-12

7 days but increased after 14 days. The sugar-acid threonic acid was significantly accumulated over time after AZA treatment and the sugar alcohol inositol. However, iditol and xylitol significantly reduced their levels after 7 days of growth. In addition, phosphoric acid, 1,4-benzenedicarboxylic acid and glucose 6-phosphate significantly decreased their levels after 7 and 14 days, whereas 4-hydroxybenzoic acid, oleic acid, putrescine, and sinapic acid were accumulated after AZA treatment.

Finally, a KEGG-based pathway analysis was conducted to further investigate the impact of AZA treatment on different metabolic pathways. The results revealed significant alterations induced by azelaic acid, which affected 45 pathways after 7 days and 49 pathways after 14 days of treatment (Supplementary Table S1). However, only 13 pathways exhibited an impact higher than 0.2 (Table 3). Among these pathways, the most significantly impacted pathways by AZA treatment were the starch and sucrose metabolism, the glycine, serine and threonine metabolism, and the arginine biosynthesis. In starch and sucrose metabolism, key metabolites such as glucose, glucose 6-phosphate and maltose were significantly altered within the network after 7 and 14 days (Figure 5A, B, respectively). On the other hand, glycine, aspartic acid and L-threonine were the most affected metabolites for glycine, serine and threonine metabolism after 7 days AZA treatment. In contrast, glycine, D-homoserine and L-threonine exhibited the highest alterations after 14 days (Figure 5A, B, respectively).

3.2.3 | Specific comparative analysis of metabolic and hormonal biosynthesis

The UHPLC/QTOF-MS metabolic profile enabled to putatively annotate more than 1700 compounds (Supplementary Table S2). Notably,

the fold-change-based heatmap of the unsupervised hierarchical clustering analysis (HCA) revealed a clear separation among sample groups, with the group of seedlings treated for 14 days showing the most pronounced separation (Figure S2A). Indeed, the clear distinction was further supported by the Supervised Orthogonal Partial Least Squares Discriminant Analysis (OPLS-DA; Figure S2B). The score plot separated the sample groups based on the 'Days of Treatment' on the first component, whereas the second component discriminated sample groups according to the 'Treatment'. The model was characterized by $R^2Y = 0.99$ (goodness-of-fit) and $Q^2Y = 0.97$ (goodness-of-prediction). The permutation test cross-validation ($N = 100$) ruled out over-fitting, and the CV-ANOVA for significance testing showed a p -value of 2.17×10^{-21} (Figure S2B). Subsequently, a VIP analysis was conducted to decipher the compounds responsible for this discrimination in response to AZA application and duration (Supplementary Table S2). The metabolite groups (VIP scores >1.2) included nitrogen-containing compounds, as well as glucosinolates, alkaloids, terpenoids, phytohormones, cytokinins and brassinosteroids, among others.

The diverse metabolites identified by Volcano plot analysis (p -value <0.05 ; FC >1.2 ; Supplementary Table S2) were grouped using pathway analysis tools from PlantCyc to observe the metabolic processes mostly affected by AZA treatment. The results revealed that AZA induced a modulation of secondary metabolism, hormones and fatty acids (Figure 6A).

Additionally, the pathway analysis tools also revealed variations in the biosynthesis of specialised metabolites (Figure 6B). Following the AZA treatment, compounds derived from fatty acids, nitrogen-containing compounds and sulphur-containing compounds showed significant accumulation at both time points (7 and 14 days). In contrast, compounds related to polyketides, pigment synthesis and

TABLE 3 Results of 'Pathway Analysis' on *Arabidopsis thaliana* seedlings, comparing untreated and azelaic acid (AZA)-treated groups for 7 and 14 days. The table displays the 13 pathways with an impact higher than 0.2. Total Cmpd: the total number of compounds in the pathway; Hits: matched number from the uploaded data; Raw P: the original P value calculated from the analysis. A False Discovery Rate (FDR) was applied to the nominal P-values. The '/' indicates $P \geq 0.05$. $n = 5$.

Pathways	Total Cmpd	Hits	AZA 7d Raw P	AZA 14d Raw P	Impact
Starch and sucrose metabolism	22	5	1.07E-10	2.57E-12	0.64
Glycine serine and threonine metabolism	33	5	6.30E-08	1.44E-07	0.59
Phenylalanine metabolism	12	1	//	3.74E-04	0.42
Arginine biosynthesis	18	6	9.79E-05	2.41E-08	0.39
Arginine and proline metabolism	32	5	1.65E-09	1.88E-08	0.39
Cyanoamino acid metabolism	29	7	1.90E-08	7.49E-08	0.36
beta-Alanine metabolism	18	3	1.70E-04	1.55E-07	0.32
Alanine aspartate and glutamate metabolism	22	6	4.13E-07	0.004927	0.26
Galactose metabolism	27	7	1.17E-07	1.72E-11	0.24
Biosynthesis of various plant secondary metabolites	29	1	8.39E-08	3.86E-06	0.24
Tryptophan metabolism	29	1	//	0.010179	0.21
Glyoxylate and dicarboxylate metabolism	29	6	3.25E-07	3.11E-06	0.20
Tyrosine metabolism	17	2	1.56E-04	3.83E-11	0.20

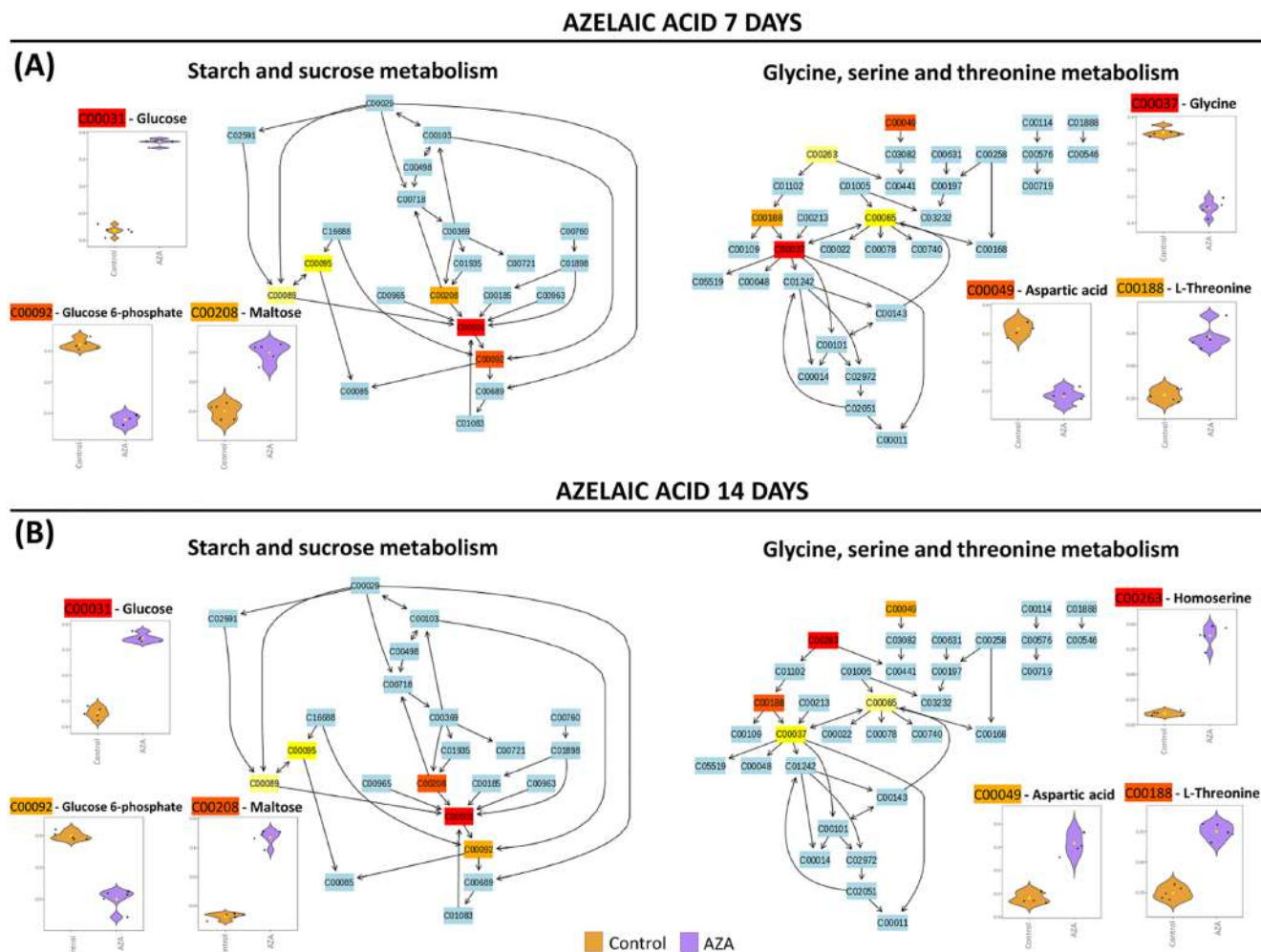


FIGURE 5 Graphical representation of enrichment pathway analysis results. (A) Two metabolic pathways strongly affected by azelaic acid after 7 days of treatment. (B) Two metabolic pathways strongly affected by azelaic acid after 14 days of treatment. Compounds in blue indicate that they are not present in the data and were added as background. In contrast, variations from yellow to red highlight metabolites with different significance levels. The violin plots represent the three metabolites strongly affected within the pathway. In the violin plots, control samples are represented in orange, and azelaic acid (AZA) samples are represented in purple. FDR-adjusted $p \leq 0.05$. $n = 5$.

terpenes were down-accumulated after 7 days but increased after 14 days of AZA treatment (Figure 6B).

Finally, the modulation of diverse phytohormones were examined, revealing that AZA treatment altered cytokinin synthesis, causing a general reduction in *trans*-zeatin-9-*N*-glucoside, dihydrozeatin-7-*N*-glucose, kinetin and kinetin-7-*N*-glucoside after both time points (7 and 14 days of treatment). In contrast, the cytokinins dihydrozeatin, dihydrozeatin-9-*N*-glucoside-*O*-glucoside, *cis*-zeatin, and *N*6-dimethylallyladenine increased their levels after 7 days of AZA treatment (Figure 7). Additionally, AZA induced an accumulation of jasmonates, i.e. (+)-7-epi-jasmonate and *cis*-tuberonic acid, with increased levels at both treatment times (Figure 7). Similarly, AZA induced a global reduction in brassinosteroids, specifically (22 R ,23 R)-22,23-dihydroxy-campest-4-en-3-one and 3-epi-6-deoxocathasterone (Figure 7). Finally, the metabolites related to auxin biosynthesis (methyl (indol-3-yl) acetate and 5-adenosyl-L-homocysteine), slightly decreased after 7 days of AZA treatment (Figure 7).

4 | DISCUSSION

The results of this study demonstrated that low concentrations of azelaic acid not only alter plant growth and development, as already observed in a previous study by Álvarez-Rodríguez et al., (2024), but also caused alterations at different levels of the *A. thaliana* metabolism. Both ionic and metabolomic approaches identified imbalances in numerous minerals and metabolites in response to the stress induced by AZA treatment. A first global comparative analysis of metabolomics data was conducted to evaluate the influence of treatment duration on the metabolite levels of azelaic acid-treated seedlings and vice versa. Pattern hunter correlation analyses revealed that glutaric acid and inositol exhibited the highest positive correlation with the treatment. This indicates that plants treated with AZA experience an upward increase in the levels of these metabolites over time. Morcol et al., (2020) reported an increment in glutaric acid levels in *Humulus lupulus* L. plants under drought stress conditions, suggesting

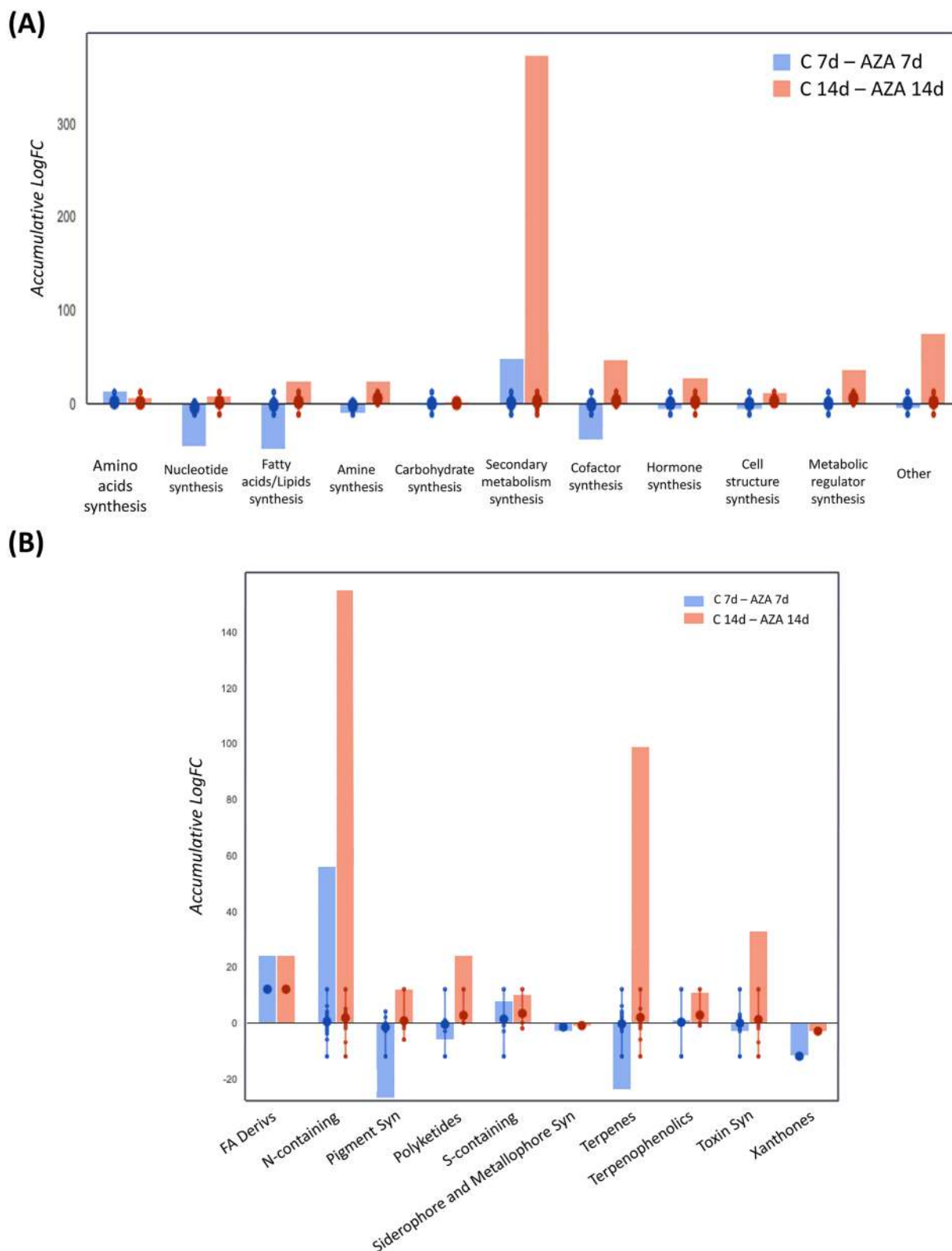


FIGURE 6 Graphical representation of significantly altered (A) metabolic processes and (B) specialized metabolite biosynthesis of *A. thaliana* seedlings untreated and treated with azelaic acid for 7 and 14 days. In both graphics, blue bars represent the accumulative LogFC of data comparisons between control and AZA-treated plants after seven days, while orange bars represent comparisons after 14 days of treatment. Positive bars indicate an increase after AZA treatment, while negative bars indicate a decrease compared to the control. n = 5.

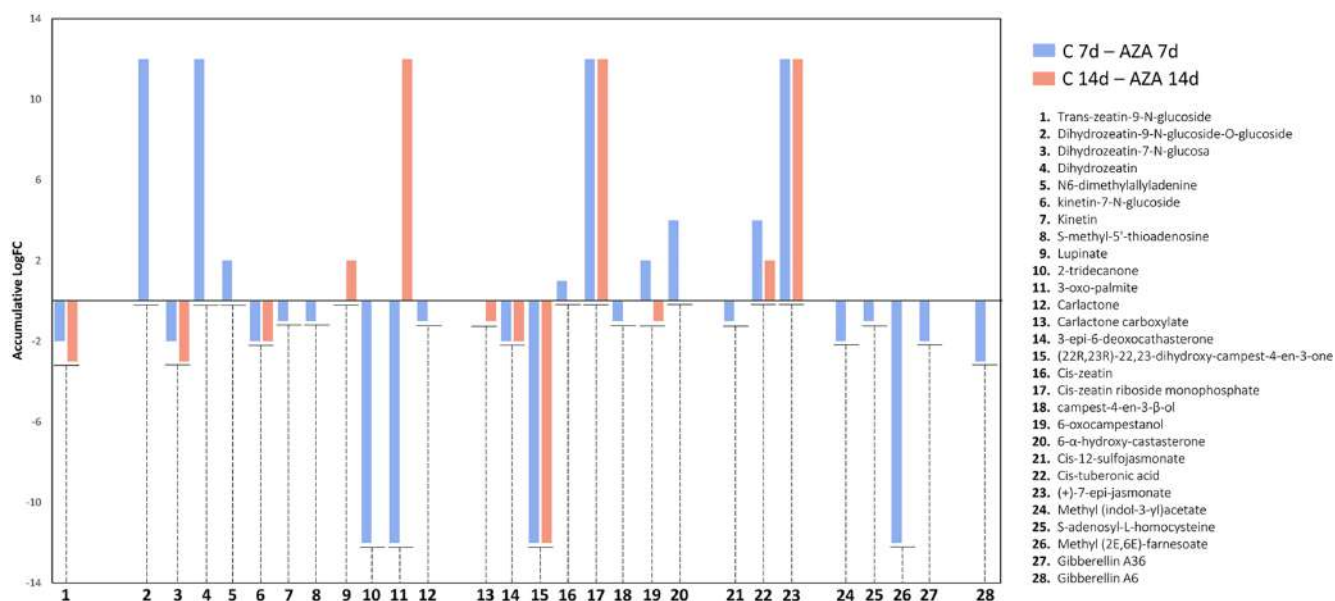


FIGURE 7 Graphical representation of significant altered hormone biosynthesis ($p \leq 0.05$) modulated in *A. thaliana* seedlings untreated and treated with azelaic acid for 7 and 14 days. In the graphic, blue bars represent data comparisons between control and AZA-treated plants after 7 days, while orange bars represent comparisons after 14 days of AZA treatment. $n = 5$.

that changes in glutaric acid content could be related to alterations in the TCA cycle, as found for one of the metabolic pathways altered after AZA treatment. Yang et al., (2017) reported that the content of glutaric acid was higher in salt-tolerant soybean subjected to salt stress in comparison with common wild soybean. Furthermore, an increase in glutaric acid content was observed in Egyptian rice under drought stress, suggesting the accumulation of this osmoprotectant as a strategy to maintain cellular osmotic adjustment (Hassanein et al., 2021). Inositol is also considered an osmoprotectant for plant protection under abiotic stress situations. It has been reported that, under salt stress conditions, inositol accumulation is related to protection against ROS (Zulfiqar et al., 2020). Hence, the accumulation of glutaric acid and inositol over time, both considered as osmoprotectants, could be a plant strategy to cope with the stress induced by AZA treatment.

Metabolomic analyses also revealed that putrescine exhibited a high positive correlation with the treatment, indicating that plants treated with AZA also experienced a significant accumulation of this metabolite over time. Putrescine is considered one of the first metabolic biomarkers, tractable through metabolomics, that is interesting for detecting potassium deficiency (Cui et al., 2020). This metabolite was found to accumulate in plants under low potassium availability (Murty et al., 1971), which is consistent with our metabolomic and ionic results. Moreover, the polyamine putrescine, as previously shown for glutaric acid and inositol, has also been reported as an osmoprotectant under osmotic stress. This polyamine has been related to mitigation of salt (K. Liu et al., 2000; Sánchez-Moreiras et al., 2009), drought (C. J. Liu et al., 2018), and other types of osmotic-related stress conditions (Chen et al., 2019), by modulating physio-biochemical traits and gene expression in stressed plants.

Moreover, the exogenous application of putrescine (Put) has been recently found to mitigate oxidative stress induced by drought (Islam et al., 2022) or salinity (Islam et al., 2021). Put-sprayed plants were more tolerant to drought and salt stress because of enhanced antioxidant enzyme activities involved in the regulation of the homeostasis of free radicals and other reactive oxygen species (Islam et al., 2022).

In contrast, Pattern hunter correlation analyses revealed that glucose 6-phosphate and aconitic acid exhibited the strongest negative linear correlations, indicating that AZA treatment led to a downward trend in the levels of these metabolites over time. The formation of glucose 6-phosphate occurs through the phosphorylation of glucose by the hexokinase1 (HXK1) enzyme, which functions as a metabolic enzyme and a glucose sensor in the glycolytic pathway (Vanderwall & Gendron, 2023). The observation that azelaic acid treatment led to a general accumulation of sugar content, whereas glucose 6-phosphate was significantly reduced over time, suggests that AZA may be affecting the proper functioning of HXK1 and, consequently, reducing glucose 6-phosphate formation.

On the other hand, plants treated with AZA experienced a significant reduction in aconitic acid content with increasing times of AZA treatment. The enzyme citrate dehydrase catalyses the dehydration of citrate to form aconitic acid. Igamberdiev and Eprintsev (2016) reported that potassium availability may influence the levels of aconitic acid in plants, as potassium stimulates the activity of the enzyme citrate dehydrase. This statement aligns with our results, as ionic analysis revealed that AZA treatment significantly reduced potassium levels, potentially influencing the formation of aconitic acid. In addition, Wang and Wu (2013) reported that TRH1, a potassium transporter, is required for auxin polar transport, and it is also implicated in the root gravitropic response, with wild-type *Arabidopsis* roots

exhibiting abnormal gravitropic behavior in response to K deficiency. This finding establishes a connection between the present study and the previous one conducted by Álvarez-Rodríguez et al., (2024). In that study, AZA was found to slow down the root gravitropic response and reduce the auxin polar transport in Arabidopsis seedlings, suggesting that AZA's mode of action could be associated with auxin imbalance, given its auxin-like properties. Consequently, alterations in potassium levels could indicate that the mode of action of AZA affects potassium homeostasis, thereby influencing the gravitropic response and the proper functioning of TRH1, thus disrupting the auxin transport system.

After 14 days of growth, ionic analysis revealed that AZA-treated seedlings also experienced a reduction in the concentration of phosphorus (P), an essential nutrient involved in diverse metabolic and physiological processes, such as cell division or phospholipid biosynthesis. As previously reported by Khan et al., (2023), insufficient P can lead to disruptions in nutrient uptake, such as reduced levels of calcium (Ca) and potassium (K). This aligns with our results, as the ionome profile showed reduced levels of Ca and K compared to the control group. Additionally, metabolomics results displayed a significant decrease in phosphoric acid levels after AZA treatment. Furthermore, plants have developed multiple physiological adaptations to cope with P deficiency. Zhang et al., (2018) reported that, under low-P conditions, plants modulate root architecture through auxin, increasing lateral root growth to enhance the surface area for the absorption of phosphorus (Nacry et al., 2005). This finding is consistent with the effects observed by Álvarez-Rodríguez et al., (2024) in the initial approach with AZA in *A. thaliana* seedlings. In addition, root exudation is another strategy employed by plants to cope with phosphorus deficiency. It has been demonstrated that plants often adjust the production and exudation of organic compounds, such as malate or citrate, to enhance the efficiency of phosphorus absorption (Irfan et al., 2020). As observed in the metabolomic profile of AZA-treated *A. thaliana* seedlings, the increase of malic acid within the roots could be considered a plant strategy to face P deficiency through enhanced exudation of malate from the roots into the soil.

Secondly, the metabolomics data were separately analyzed at 7 and 14 days of treatment to further examine the specific alterations occurring in the plant metabolome of *A. thaliana* seedlings individually. The *t*-tests conducted on the metabolomic data after 7 and 14 days of AZA treatment revealed that the metabolomic profile of AZA-treated seedlings experienced a general accumulation of sugar content. Gibson (2005) reported that elevated sugar levels can stimulate the formation of adventitious roots in Arabidopsis, which was already noted by Álvarez-Rodríguez et al., (2024) in AZA-treated Arabidopsis roots. Accumulation of soluble sugars, considered as osmoprotectants, enhances plant tolerance to diverse abiotic stresses, such as drought, salt or heat stress (Afzal et al., 2021). After AZA treatment, glucose and maltose have been reported as the metabolites mostly affected within the 'starch and sucrose metabolism' metabolism pathway. A significant increase in glucose and fructose levels was observed in *A. thaliana* seedlings treated with the natural compound rosmarinic acid, suggesting a plant response to oxidative stress (Araniti

et al., 2018). Likewise, Ibrahim and Abdellatif (2016) reported that exogenous foliar application of maltose could improve water stress tolerance in wheat plants. Hence, *A. thaliana* seedlings could face the stress situation caused by AZA treatment by inducing sugar accumulation within the plant. De Marco et al., (2024) recently reported exogenous application of indole-3-acetic acid (IAA) induced starch accumulation in the algae *C. reinhardtii*. In addition, glucose has been reported to reduce meristem size, thereby inhibiting auxin polar transport during Arabidopsis root elongation (Serrano et al., 2023). These findings help to establish a connection between this study and the preceding one conducted by Álvarez-Rodríguez et al., (2024) on AZA-treated Arabidopsis seedlings. Álvarez-Rodríguez et al., (2024), suggested that AZA competes with auxin for the binding site TIR1 (with the receptor Transport Inhibitor Response 1), acting as an auxinic herbicide. Consequently, if AZA behaves similarly to auxin, the external application of AZA, would induce starch and glucose accumulation as recorded, which would affect auxin polar transport and root architecture, as previously reported by Álvarez-Rodríguez et al., (2024).

Ionic analysis also revealed that AZA significantly reduced the levels of magnesium (Mg). Kumar Tewari et al., (2006) investigated the response of mulberry plants to Mg deficiency, demonstrating that low levels of Mg induced oxidative stress and elicited antioxidative responses. In addition, Kobayashi and Tanoi (2015) reported that long-term Mg deficiency could lead to several disruptions in plant metabolism, such as the production of reactive oxygen species (ROS) or starch accumulation, since an adequate concentration of Mg is required for the proper transport of sucrose within the phloem (Hermans & Verbruggen, 2005). Hence, the starch accumulation observed after AZA treatment could be directly connected to the Mg deficiency.

Moreover, a general accumulation of the amino acids lysine, GABA, threonine, proline and glutamine was noticed. However, serine levels were significantly lower after AZA treatment. This aligns with the results of the pathway analysis, revealing that 'Glycine serine and threonine metabolism' and 'Alanine aspartate and glutamate metabolism' are two of the most impacted pathways after AZA treatment. Under abiotic stress conditions, the accumulation of diverse amino acids plays a pivotal role in inducing stress tolerance (Joshi et al., 2010). Indeed, it has been reported that under amino acid accumulations, these metabolites are often catabolized into the tricarboxylic acid (TCA) cycle to obtain energy for the plant in response to a stress situation (Galili et al., 2016; Kirma et al., 2012). Hence, the accumulation of amino acids could be related to the increased energy demand required for plant growth in response to the stress induced by AZA treatment. Moreover, proline is known to be one of the most important compatible osmolytes and one of the major amino acids related to protection under diverse abiotic stresses, conferring tolerance against drought, metal toxicity, salt stress or high temperature (Sánchez-Moreiras et al., 2009; Teixeira et al., 2020).

In addition, AZA induced accumulation of the organic acids fumaric, shikimic, succinic and gluconic acids. Shikimic acid is considered a central metabolite implicated in the formation of diverse specialized

metabolites, including aromatic amino acids and phenolic compounds (Marchiosi et al., 2020). These specialized metabolites play crucial roles within the plant, acting as antioxidants, signaling agents, or participating in plant defense against various stresses (Santos-Sánchez et al., 2019; Vieites-Álvarez et al., 2023). The increase in shikimic acid content is consistent with the significant rise in the synthesis of specialized metabolites observed in the metabolomic profile of AZA-treated plants. This increase in shikimic acid may be correlated with the modulation of tryptophan and tyrosine, two aromatic amino acids synthesized through the shikimate pathway, in which shikimic acid acts as intermediate (S. Wu et al., 2022). Indeed, the aromatic acids produced by the shikimate pathway are known precursors of nitrogen-containing compounds, terpenes and sulphur-containing specialized metabolites (Jan et al., 2021). As well, these specialized metabolites were found to be upregulated in the metabolomic profile of *A. thaliana* seedlings after AZA treatment, and plants regularly produce them as a protection strategy against biotic or abiotic stress. The group of sulphur-containing specialized metabolites includes about 200 compounds that are directly or indirectly connected to the plant defense system. They are important for plant health, as sufficient levels of sulphur are essential for the proper utilization of nitrogen by the plant (Bloem et al., 2007). Jan et al., (2021) reported that sulphur-containing compounds are commonly synthesized in response to diverse environmental stresses. Hence, the accumulation of organic acids in response to AZA treatment is directly connected with the increase in the synthesis of diverse specialized metabolites, such as nitrogen-containing compounds, terpenes and sulphur-containing compounds.

Finally, AZA treatment induced an accumulation of jasmonates. Jasmonates (JA) play a crucial role in plant growth and development. Huang et al., (2017) reported that JA has an inhibitory effect on Arabidopsis plant growth, serving as a strategy to enhance plant survival in defense against various stresses. Evidence suggested a crosstalk between jasmonates and auxin in coordinating plant responses to diverse stimuli (Grunewald et al., 2009). Tiryaki and Staswick (2002) further reported that auxin stimulates the transcript levels of jasmonates biosynthesis genes in Arabidopsis plants. In contrast, Arabidopsis plants treated with methyl-JA showed a significant increase in free IAA levels (Dombrecht et al., 2007). Consequently, the results obtained in this study are in accordance with the primary hypothesis regarding the mode of action of AZA in plant metabolism. AZA acts as an auxin molecule by competing with the TIR1 receptor for the binding site, promoting the accumulation of free auxin in the upper parts of the root (Álvarez-Rodríguez et al., 2024). This, in turn, would stimulate the synthesis of jasmonates, as observed in our study. On the contrary, AZA induced a global reduction in brassinosteroid (BRs) levels. Imbalances in BR levels in plants have been reported to alter primary root growth and development, with mutants lacking BR compounds developing short roots (Chaiwanon & Wang, 2015; Planas-Riverola et al., 2019). Consequently, the increase in jasmonates and the reduction in brassinosteroid levels are in line with the observed alterations in plant root growth in *A. thaliana* seedlings treated with AZA, as previously reported by Álvarez-Rodríguez et al., (2024). These results support the hypothesis of auxin imbalance in the mode of

action of azelaic acid. Future studies will explore the herbicidal potential of AZA in a broader range of plant species, ideally in soil-grown conditions, to better assess its applicability in agriculture. Our work lays a critical foundation for understanding AZA's mode of action and opens avenues for its potential use in agricultural weed management.

5 | CONCLUSIONS

The results of this study demonstrate that AZA causes stress in *A. thaliana* seedlings, inducing a general accumulation of diverse osmoprotectants: sugars (glucose, mannose, xylose, etc.), amino acids (lysine, GABA, threonine, glutamine, etc.) and organic acids (glutaric acid, fumaric acid, succinic acid, etc.), all strongly related to oxidative stress on plant metabolism. Additionally, ionic analysis revealed that AZA-treated seedlings experienced phosphorus and magnesium deficiency. Azelaic acid treatment also led to the accumulation of putrescine over time, which is considered a metabolic biomarker for detecting potassium deficiency. The metabolic profile revealed increased synthesis of diverse specialized metabolites, such as nitrogen- and sulphur-containing compounds. Finally, AZA caused an imbalance in the levels of various phytohormones, such as jasmonates and brassinosteroids. The findings of this study support the primary hypothesis regarding the mode of action of AZA, suggesting that AZA functions as an auxinic herbicide by competing with auxin for the auxin-binding site TIR1. This competition leads to an increase in starch and jasmonate levels, contributing to disruptions in potassium homeostasis. Consequently, these alterations impact the auxin transport system, root architecture and gravitropic root response.

AUTHOR CONTRIBUTIONS

The experimental conceptualization was done by S.Á.-R., F.A., A.M.S.-M. and L.L. The experimental methodology was performed by S.Á.-R., B.S. and G.L.. The software and formal analysis was carried out by S.Á.-R. and B.S.. The original draft preparation was done by S.Á.-R. and B.S. The draft supervision was done by F.A., A.M.S.-M. and L.L. The funding was obtained by F.A. and A.M.S.-M.

ACKNOWLEDGEMENTS

Sara Álvarez-Rodríguez gratefully acknowledges the financial support from the Xunta de Galicia. We also thank the University of Vigo for covering the open access publication fees.

FUNDING INFORMATION

The results of this study are part of the I + D + I project RT12018-094716-B-100 funded by MCIN/AEI/10.13039/501100011033, and part of the European EU-Horizon project "AGROSUS: AGRO-ecological strategies for SUSTainable weed management in key European crop" under grant agreement number 101084084. Sara Álvarez-Rodríguez was supported by a predoctoral fellowship of the Galician Government (ED481A-2021/328). Funding for open access charge: Universidade de Vigo/CRUE-CISUG.

DATA AVAILABILITY STATEMENT

The authors confirm that the raw data supporting this article's findings are included in its Supplementary Material section.

ORCID

Sara Álvarez-Rodríguez  <https://orcid.org/0000-0001-7064-4272>

Biancamaria Senizza  <https://orcid.org/0000-0001-5807-7113>

Fabrizio Araniti  <https://orcid.org/0000-0002-4983-4116>

Luigi Lucini  <https://orcid.org/0000-0002-5133-9464>

Adela M. Sánchez-Moreiras  <https://orcid.org/0000-0002-0771-9259>

REFERENCES

- Afzal, S., Chaudhary, N., & Singh, N.K. (2021) Role of soluble sugars in metabolism and sensing under abiotic stress. In T. Aftab & K. R. Hakeem (Eds.), *Plant Growth Regulators* (pp. 305–334). Springer International Publishing.
- Álvarez-Rodríguez, S., Alvite, C.M., Reigosa, M.J., Sánchez-Moreiras, A.M., & Araniti, F. (2023a) Application of indole-alkaloid harmaline induces physical damage to photosystem II antenna complexes in adult plants of *Arabidopsis thaliana* (L.) Heynh. *Journal of Agricultural and Food Chemistry*, 71(15), 6073–6086.
- Álvarez-Rodríguez, S., Araniti, F., Teijeira, M., Reigosa, M.J., & Sánchez-Moreiras, A.M. (2024) Azelaic acid can efficiently compete for the auxin binding site TIR1, altering auxin polar transport, gravitropic response, and root growth and architecture in *Arabidopsis thaliana* roots. *Plant Physiology and Biochemistry*, 210, 108592.
- Álvarez-Rodríguez, S., Spinozzi, E., Sánchez-Moreiras, A.M., López-González, D., Ferrati, M., Lucchini, G., Maggi, F., Petrelli, R., & Araniti, F. (2023b) Investigating the phytotoxic potential of *Carlina acaulis* essential oil against the weed *Bidens pilosa* through a physiological and metabolomic approach. *Industrial Crops and Products*, 203, 117149.
- Araniti, F., Costas-Gil, A., Cabeiras-Freijanes, L., Lupini, A., Sunseri, F., Reigosa, M.J., Abenavoli, M.R., & Sánchez-Moreiras, A.M. (2018) Rosmarinic acid induces programmed cell death in *Arabidopsis* seedlings through reactive oxygen species and mitochondrial dysfunction. *Plos one*, 13(12), e0208802.
- Araniti, F., Miras-Moreno, B., Lucini, L., Landi, M., & Abenavoli, M.R. (2020) Metabolomic, proteomic and physiological insights into the potential mode of action of thymol, a phytotoxic natural monoterpenoid phenol. *Plant Physiology and Biochemistry*, 153, 141–153.
- Bloem, E., Haneklaus, S., Salac, I., Wickenhäuser, P., & Schnug, E. (2007) Facts and fiction about sulfur metabolism in relation to plant-pathogen interactions. *Plant Biology*, 9(5), 596–607.
- Chaiwanon, J., & Wang, Z.Y. (2015) Spatiotemporal brassinosteroid signaling and antagonism with auxin pattern stem cell dynamics in *Arabidopsis* roots. *Current Biology*, 25(8), 1031–1042.
- Chen, D., Shao, Q., Yin, L., Younis, A., & Zheng, B. (2019) Polyamine function in plants: metabolism, regulation on development, and roles in abiotic stress responses. *Frontiers in Plant Science*, 9, 1945.
- Cui, J., Pottosin, I., Lamade, E., & Tcherkez, G. (2020) What is the role of putrescine accumulated under potassium deficiency? *Plant, Cell & Environment*, 43(6), 1331–1347.
- Dayan, F.E., & Duke, S.O. (2020) Discovery for new herbicide sites of action by quantification of plant primary metabolite and enzyme pools. *Engineering*, 6(5), 509–514.
- De Marco, M.A., Curatti, L., & Martínez-Noël, G.M.A. (2024) High auxin disrupts expression of cell-cycle genes, arrests cell division and promotes accumulation of starch in *Chlamydomonas reinhardtii*. *Algal Research*, 78, 103419.
- Dombrecht, B., Xue, G.P., Sprague, S.J., Kirkegaard, J.A., Ross, J.J., Reid, J.B., Fitt, G.P., Sewelam, N., Schenk, P.M., Manners, J.M., & Kazan, K. (2007) Myc2 differentially modulates diverse jasmonate-dependent functions in *Arabidopsis*. *The Plant Cell*, 19(7), 2225–2245.
- Dong, J., Chang, M., Li, C., Dai, D., & Gao, Y. (2019) Allelopathic effects and potential active substances of *Ceratophyllum demersum* L. on *Chlorella vulgaris* Beij. *Aquatic Ecology*, 53(4), 651–663.
- Galili, G., Amir, R., & Fernie, A.R. (2016) The regulation of essential amino acid synthesis and accumulation in plants. *Annual Review of Plant Biology*, 67(1), 153–178.
- Gibson, S.I. (2005) Control of plant development and gene expression by sugar signaling. *Current Opinion in Plant Biology*, 8(1), 93–102.
- Grunewald, W., Vanholme, B., Pauwels, L., Plovie, E., Inzé, D., Gheysen, G., & Goossens, A. (2009) Expression of the *Arabidopsis* jasmonate signalling repressor JAZ1 / TIFY10A is stimulated by auxin. *EMBO Reports*, 10(8), 923–928.
- Hassanein, A., Ibrahim, E., Abou Ali, R., & Hashem, H. (2021) Differential metabolic responses associated with drought tolerance in Egyptian rice. *Journal of Applied Biology & Biotechnology*, 9(4), 37–46.
- Hermans, C., & Verbruggen, N. (2005) Physiological characterization of Mg deficiency in *Arabidopsis thaliana*. *Journal of Experimental Botany*, 56(418), 2153–2161.
- Hirabayashi, M., Ozaki, T., & Matsuo, M. (2001) The phytotoxicity to tobacco plants of short-chain carboxylic acids at atmospheric concentration levels in urban areas. *Environmental Technology*, 22(3), 301–305.
- Huang, H., Liu, B., Liu, L., & Song, S. (2017) Jasmonate action in plant growth and development. *Journal of Experimental Botany*, 68(6), 1349–1359.
- Ibrahim, H.A., & Abdellatif, Y. M.R. (2016) Effect of maltose and trehalose on growth, yield and some biochemical components of wheat plant under water stress. *Annals of Agricultural Sciences*, 61(2), 267–274.
- Igamberdiev, A.U., & Eprntsev, A.T. (2016) Organic acids: the pools of fixed carbon involved in redox regulation and energy balance in higher plants. *Frontiers in Plant Science*, 7.
- Irfan, M., Aziz, T., Maqsood, M.A., Bilal, H.M., Siddique, K.H.M., & Xu, M. (2020) Phosphorus (P) use efficiency in rice is linked to tissue-specific biomass and P allocation patterns. *Scientific Reports*, 10(1), 4278.
- Islam, M.J., Uddin, M.J., Hossain, M.A., Henry, R., Begum, Mst. K., Sohel, Md. A.T., Mou, M.A., Ahn, J., Cheong, E.J., & Lim, Y.S. (2022) Exogenous putrescine attenuates the negative impact of drought stress by modulating physio-biochemical traits and gene expression in sugar beet (*Beta vulgaris* L.). *Plos one*, 17(1), e0262099.
- Islam, Md. J., Ryu, B.R., Azad, Md. O.K., Rahman, Md. H., Rana, Md. S., Lim, J.D., & Lim, Y.S. (2021) Exogenous putrescine enhances salt tolerance and ginsenosides content in Korean ginseng (*Panax ginseng* Meyer) sprouts. *Plants*, 10(7), 1313.
- Jan, R., Asaf, S., Numan, M., Lubna, & Kim, K.M. (2021) Plant secondary metabolite biosynthesis and transcriptional regulation in response to biotic and abiotic stress conditions. *Agronomy*, 11(5), 968.
- Joshi, V., Joung, J.G., Fei, Z., & Jander, G. (2010) Interdependence of threonine, methionine and isoleucine metabolism in plants: Accumulation and transcriptional regulation under abiotic stress. *Amino Acids*, 39(4), 933–947.
- Khan, F., Siddique, A.B., Shabala, S., Zhou, M., & Zhao, C. (2023) Phosphorus plays key roles in regulating plants' physiological responses to abiotic stresses. *Plants*, 12(15), 2861.
- Kirma, M., Araujo, W.L., Fernie, A.R., & Galili, G. (2012) The multifaceted role of aspartate-family amino acids in plant metabolism. *Journal of Experimental Botany*, 63(14), 4995–5001.
- Kobayashi, N., & Tanoi, K. (2015) Critical issues in the study of magnesium transport systems and magnesium deficiency symptoms in plants. *International Journal of Molecular Sciences*, 16(9), 23076–23093.
- Kumar Tewari, R., Kumar, P., & Nand Sharma, P. (2006) Magnesium deficiency induced oxidative stress and antioxidant responses in mulberry plants. *Scientia Horticulturae*, 108(1), 7–14.
- Kumari, A., Das, P., Parida, A.K., & Agarwal, P.K. (2015) Proteomics, metabolomics, and ionomics perspectives of salinity tolerance in halophytes. *Frontiers in Plant Science*, 6.

- Lisec, J., Schauer, N., Kopka, J., Willmitzer, L., & Fernie, A.R. (2006) Gas chromatography mass spectrometry-based metabolite profiling in plants. *Nature Protocols*, 1(1), 387–396.
- Liu, C.J., Wang, H.R., Wang, L., Han, Y.Y., Hao, J.H., & Fan, S.X. (2018) Effects of different types of polyamine on growth, physiological and biochemical nature of lettuce under drought stress. *IOP Conference Series: Earth and Environmental Science*, 185, 012010.
- Liu, K., Fu, H., Bei, Q., & Luan, S. (2000) Inward potassium channel in guard cells as a target for polyamine regulation of stomatal movements. *Plant Physiology*, 124(3), 1315–1326.
- López-González, D., Graña, E., Teijeira, M., Verdeguer, M., Reigosa, M.J., Sánchez-Moreiras, A.M., & Araniti, F. (2023) Similarities on the mode of action of the terpenoids citral and farnesene in *Arabidopsis* seedlings involve interactions with DNA binding proteins. *Plant Physiology and Biochemistry*, 196, 507–519.
- Ma, Y., Chun, J., Wang, S., & Chen, F. (2011) Allelopathic potential of *Jatropha curcas*. *African Journal of Biotechnology*, 10(56), 11932–11942.
- Marchiosi, R., Dos Santos, W.D., Constantin, R.P., De Lima, R.B., Soares, A.R., Finger-Teixeira, A., Mota, T.R., De Oliveira, D.M., Foletto-Felipe, M.D.P., Abrahão, J., & Ferrarese-Filho, O. (2020) Biosynthesis and metabolic actions of simple phenolic acids in plants. *Phytochemistry Reviews*, 19(4), 865–906.
- Misra, B.B., Das, V., Landi, M., Abenavoli, M.R., & Araniti, F. (2020) Short-term effects of the allelochemical umbelliferone on *Triticum durum* L. metabolism through GC-MS based untargeted metabolomics. *Plant Science*, 298, 110548.
- Morcol, T.B., Wysocki, K., Sankaran, R.P., Matthews, P.D., & Kennelly, E.J. (2020) UPLC-QToF-MS^E Metabolomics reveals changes in leaf primary and secondary metabolism of hop (*Humulus lupulus* L.) plants under drought stress. *Journal of Agricultural and Food Chemistry*, 68(49), 14698–14708.
- Murty, K.S., Smith, T.A., & Bould, C. (1971) The relation between the putrescine content and potassium status of black currant leaves. *Annals of Botany*, 35(3), 687–695.
- Nacry, P., Canivenc, G., Muller, B., Azmi, A., Van Onckelen, H., Rossignol, M., & Dumas, P. (2005) A role for auxin redistribution in the responses of the root system architecture to phosphate starvation in *Arabidopsis*. *Plant Physiology*, 138(4), 2061–2074.
- Pita-Barbosa, A., Ricachenevsky, F.K., Wilson, M., Dottorini, T., & Salt, D.E. (2019) Transcriptional plasticity buffers genetic variation in zinc homeostasis. *Scientific Reports*, 9(1), 19482.
- Planas-Riverola, A., Gupta, A., Betegón-Putze, I., Bosch, N., Ibañez, M., & Caño-Delgado, A.I. (2019) Brassinosteroid signaling in plant development and adaptation to stress. *Development*, 146(5), dev151894.
- Qu, R., He, B., Yang, J., Lin, H., Yang, W., Wu, Q., Li, Q.X., & Yang, G. (2021) Where are the new herbicides? *Pest Management Science*, 77(6), 2620–2625.
- Salam, U., Ullah, S., Tang, Z.H., Elateeq, A.A., Khan, Y., Khan, J., Khan, A., & Ali, S. (2023) Plant metabolomics: An overview of the role of primary and secondary metabolites against different environmental stress factors. *Life*, 13(3), 706.
- Salek, R.M., Steinbeck, C., Viant, M.R., Goodacre, R., & Dunn, W.B. (2013) The role of reporting standards for metabolite annotation and identification in metabolomic studies. *GigaScience*, 2(1), 13.
- Sánchez-Moreiras, A.M., Pedrol, N., González, L., & Reigosa, M.J. (2009) 2-3 H-Benzoxazolinone (BOA) induces loss of salt tolerance in salt-adapted plants. *Plant Biology*, 11(4), 582–590.
- Sansone, S.A., Schober, D., Atherton, H.J., Fiehn, O., Jenkins, H., Rocca-Serra, P., Rubtsov, D.V., Spasic, I., Soldatova, L., Taylor, C., Tseng, A., Viant, M.R., & Ontology Working Group Members. (2007) Metabolomics standards initiative: ontology working group work in progress. *Metabolomics*, 3, 249–256.
- Santos-Sánchez, N.F., Salas-Coronado, R., Hernández-Carlos, B., & Villanueva-Cañongo, C. (2019) Shikimic acid pathway in biosynthesis of phenolic compounds. In *Plant physiological aspects of phenolic compounds* (pp. 1–15). IntechOpen.
- Serrano, A., Kuhn, N., Restovic, F., Meyer-Regueiro, C., Madariaga, M., & Arce-Johnson, P. (2023) The glucose-related decrease in polar auxin transport during ripening and its possible role in grapevine berry coloring. *Journal of Plant Growth Regulation*, 42(1), 365–375.
- Slama, I., Abdelly, C., Bouchereau, A., Flowers, T., & Savouré, A. (2015) Diversity, distribution and roles of osmoprotective compounds accumulated in halophytes under abiotic stress. *Annals of Botany*, 115(3), 433–447.
- Spaggiari, C., Annunziato, G., Spadini, C., Montanaro, S.L., Iannarelli, M., Cabassi, C.S., & Costantino, G. (2023) Extraction and quantification of azelaic acid from different wheat samples (*Triticum durum* Desf.) and evaluation of their antimicrobial and antioxidant activities. *Molecules*, 28(5), 2134.
- Teixeira, W.F., Soares, L.H., Fagan, E.B., Da Costa Mello, S., Reichardt, K., & Dourado-Neto, D. (2020) Amino acids as stress reducers in soybean plant growth under different water-deficit conditions. *Journal of Plant Growth Regulation*, 39(2), 905–919.
- Tiryaki, I., & Staswick, P.E. (2002) An *Arabidopsis* mutant defective in jasmonate response is allelic to the auxin-signaling mutant *axr1*. *Plant Physiology*, 130(2), 887–894.
- Vanderwall, M., & Gendron, J.M. (2023) HEXOKINASE1 and glucose-6-phosphate fuel plant growth and development. *Development*, 150(20), dev202346.
- Vieites-Álvarez, Y., Otero, P., López-González, D., Prieto, M.A., Simal-Gandara, J., Reigosa, M.J., Hussain, M.I., & Sánchez-Moreiras, A.M. (2023) Specialized metabolites accumulation pattern in buckwheat is strongly influenced by accession choice and co-existing weeds. *Plants*, 12(13), 2401.
- Wang, Y., & Wu, W.H. (2013) Potassium transport and signaling in higher plants. *Annual Review of Plant Biology*, 64(1), 451–476.
- Wu, H.S., Liu, Y.D., Zhao, G.M., Chen, X.Q., Yang, X.N., & Zhou, X.D. (2011) Succinic acid inhibited growth and pathogenicity of *in vitro* soil-borne fungus *Fusarium oxysporum* f. sp. *Niveum*. *Acta Agriculturae Scandinavica, Section B - Plant Soil Science*, 61(5), 404–409.
- Wu, S., Chen, W., Lu, S., Zhang, H., & Yin, L. (2022) Metabolic engineering of shikimic acid biosynthesis pathway for the production of shikimic acid and its branched products in microorganisms: advances and prospects. *Molecules*, 27(15), 4779.
- Yang, D., Zhang, J., Li, M., & Shi, L. (2017) Metabolomics analysis reveals the salt-tolerant mechanism in Glycine soja. *Journal of Plant Growth Regulation*, 36(2), 460–471.
- Zhang, C., Simpson, R.J., Kim, C.M., Warthmann, N., Delhaize, E., Dolan, L., Byrne, M.E., Wu, Y., & Ryan, P.R. (2018) Do longer root hairs improve phosphorus uptake? Testing the hypothesis with transgenic *Brachypodium distachyon* lines overexpressing endogenous RSL genes. *New Phytologist*, 217(4), 1654–1666.
- Zulfiqar, F., Akram, N.A., & Ashraf, M. (2020) Osmoprotection in plants under abiotic stresses: New insights into a classical phenomenon. *Planta*, 251(1), 3.

SUPPORTING INFORMATION

Additional supporting information can be found online in the Supporting Information section at the end of this article.

How to cite this article: Álvarez-Rodríguez, S., Senizza, B., Araniti, F., Lucini, L., Lucchini, G. & Sánchez-Moreiras, A.M. (2024) Evaluating the effects of azelaic acid in the metabolism of *Arabidopsis thaliana* seedlings through untargeted metabolomics and ionomics approaches. *Physiologia Plantarum*, 176(5), e14550. Available from: <https://doi.org/10.1111/pp1.14550>